

Fatigue Strength Evaluation of Notched Specimens in Whisker - Fiber Reinforced Composite Materials

Kim Yun - Hae*

노치를 갖는 휘스커 纖維強化複合材料의 疲勞強度評價



탄화규소 휘스커섬유강화복합재료(SiC/6061-T6)의 평활재 및 노치재를 이용하여 회전굽힘피로시험을 행하고 시험편 표면의 레프리카에 의한 연속 관찰과 선형노치역학의 개념에 근거한 정리를 통하여 다음과 같은 결과를 얻었다.

(1) 휘스커섬유강화복합재료에서 휘스커섬유가 풍부한 영역과 휘스커섬유가 빈약한 영역이 층상으로 존재하며, 피로균열은 그러한 부분의 경계부근의 휘스커端(Whisker fiber end)에서 발생한다. 한편, 매트릭스인 알루미늄합금(6061-T6)에 있어서 균열은 결함으로부터 발생하며 전단형으로 전파하여 간다.

(2) 휘스커섬유강화복합재료의 경우, 균열발생이 점발생적(Point initiation type)이며 (그림8), 노치에 대해 민감하다. 그러나 K_t , $\sigma_{w1} / \sigma_{w0} - 1$ ρ 의 관계에서 노치에 대한 둔감한 것으로 나타난 것은 통계적 인자에 의해 평활재의 피로한도가 낮게 나타나고 있기 때문이다.

Nomenclature

t : notch depth(mm)

ρ : notch root radius(mm)

K_t : stress concentration factor

* Department of Materials Engineering, Korea Maritime University, Pusan, 606, Korea

- σ_{w1} : limiting stress for crack initiation
 σ_{w2} : limiting stress for fracture in the range of non - propagating crack existing
 σ_{w0} : fatigue limit of plain specimen
 σ_{max} : maximum elastic stress
 σ_a : stress amplitude

1. Introduction

In recent years, the need for lighter materials with high specific strength and stiffnesses has led to the development of numerous composite materials as serious competitors to traditional engineering alloy. In particular, silicon carbide whisker - fiber reinforced aluminum alloy is especially attractive as a structural material because of its superior specific strength, specific elastic modulus, corrosion fatigue behavior and wear resistance compared with the corresponding wrought aluminum alloys[1 - 2]. Silicon carbide is also chemically compatible with aluminum and forms an adequate bond with the matrix without developing intermetallic phases. It is applicable to a variety of machined components and can be produced as extrusion, forgings and rolling. There are many studies[3 - 13] on the mechanical properties, fracture toughness, fatigue properties and whisker volume fraction.

For example, W. A. Logsdon and P.K. Liaw[5] showed that the silicon carbide whisker - fiber reinforced aluminum alloy where the discontinuous whisker - fibers were combined in an aluminum alloy with a fiber content of 25%(by weight) demonstrated increased yield and ultimate strengths, substantially inferior ductility and fracture toughness, a lower crack propagation resistance and essentially equivalent values of threshold stress intensity factor range compared with the corresponding wrought aluminum alloys. K. Hirano[11] also showed that the silicon carbide whisker - fiber reinforced aluminum alloy is not always effective to improve fracture toughness for high strength aluminum alloy, and instead degrades the fracture toughness. There are few studies, however, on the fatigue characteristics based on the small fatigue crack nucleation and propagation of plain specimens through successive observation using the plastic replica method, and fatigue strengths of notched specimens.

In this study, rotating - bending fatigue testes for the SiC whisker fiber reinforced 6061 - T6 aluminum alloy and 6061 - T6 aluminum alloy made by powder metallurgy were carried out to investigate the fatigue characteristics of plain and notched specimens at room temperature.

The fatigue mechanisms in both materials were clarified through successive observations. The results were discussed based on linear notch mechanics.

2. Linear Notch Mechanics

In most cases, the failure or fracture of machines and structures is brought on by the localized damage of the part where the stress concentration due to the existence of a crack or a notch occurs. On the other hand, it is well known that the elastic maximum stress σ_{max} is not enough to predict the failure or fracture. Therefore, it is very important to evaluate the severity of the part having a crack or a notch.

Concerning a crack, linear fracture mechanics[14] can play an important role to predict the fracture or yield in the neighborhood of a crack tip. That is, stress intensity factor is the effective measure of severity controlling the localized damage in a crack. However, concerning a notch, the concept corresponding to linear fracture mechanics has not been discussed fully until now.

In general, a crack appears necessarily before any kind of fracture. Therefore, it may be considered that linear fracture mechanics is sufficient in treating all kinds of fracture problems. However, many notch problems[15,16] can not be treated correctly without considering the characteristics of notches. Linear notch mechanics[17,18] should be defined as an engineering method which treats the notch problem by elastic stress fields alone. Similarly, linear fracture mechanics is defined as an engineering method which treats the crack problems by elastic stress fields alone.

If the values of K_I in two cracked bodies are equal to each other, the elastic stress fields

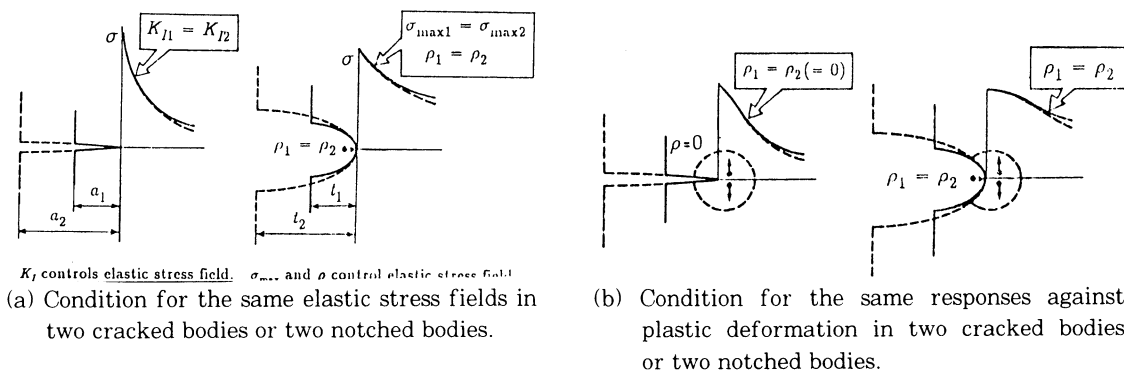


Fig. 1 Same elastic fields and same responses.

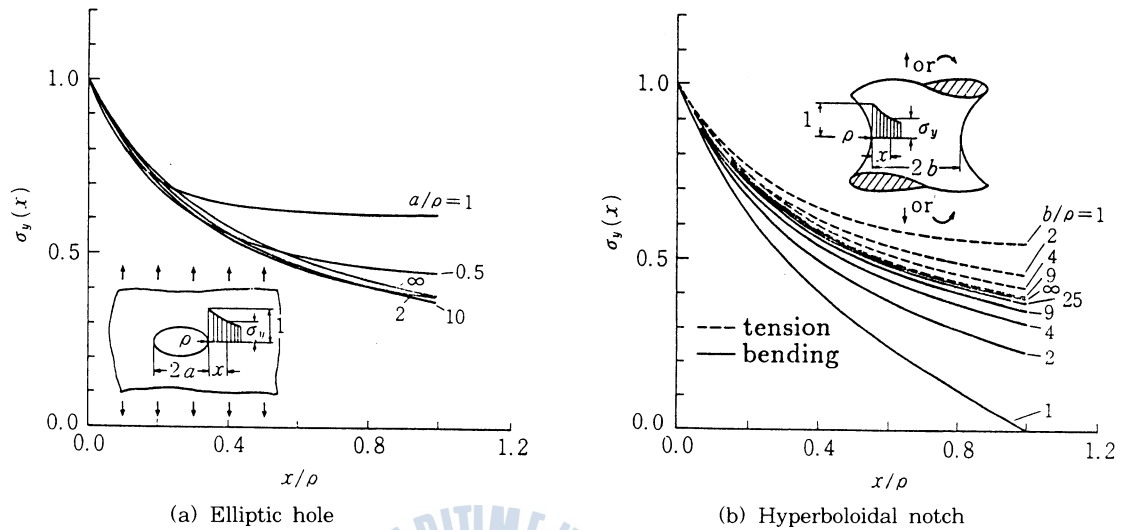


Fig. 2 Elastic stress field near the notch root is mainly determined by the values of σ_{max} and ρ alone.

near the crack tips are equal to each other in two cracked bodies, independent of crack size or the other geometrical conditions (Fig. 1(a)). There is a similar situation for notches [16]. That is, if the values of the elastic maximum stress σ_{max} and notch root radius ρ in two notched bodies are equal to each other respectively, the elastic stress fields near the notch roots are equal to each other in the two notched bodies, independent of notch depth or the other geometrical conditions [Fig. 1(a), Fig. 2].

The same elastic stress fields do not necessarily assure the occurrence of the same localized damage, because the localized damage (fatigue crack initiation, brittle fracture, local yields etc.) is usually accompanied by plastic deformation and the same elastic stress fields do not necessarily assure the occurrence of the same plastic deformations (the same elastic-plastic

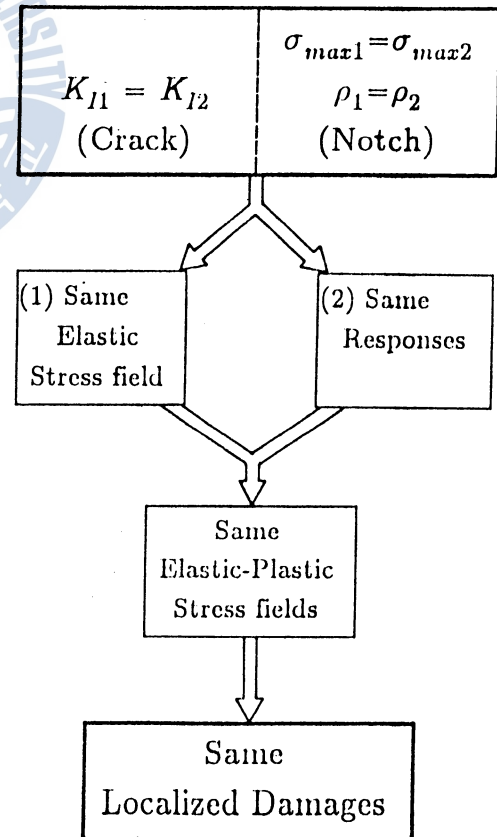


Fig. 3 Condition for causing the same localized damages in two cracked bodies or two notched bodies.

stress fields).

The reason why the same elastic stress fields assure the occurrence of the same localized damage is that the conditions for the same elastic stress fields include the condition for the same responses against plastic deformation, as shown in Fig.1(b). The same responses against plastic deformation mean the occurrence of the same additional stress fields due to a given amount of plastic deformation at a given place in two cracked or two notched bodies. The situations are shown schematically in Fig.1(b). The same elastic stress fields and the same responses against plastic deformation assure the occurrence of the same elastic-plastic stress fields in two cracked bodies or in two notched bodies. The same elastic-plastic stress fields assure the occurrence of the same localized damage. The interrelation of these facts is shown in Fig. 3. From the above discussion, it is concluded that the measure of severity controlling the localized damage is the value of K_I in a crack and the value of σ_{max} and notch root radius ρ in a notch. The former is the measure of severity in linear fracture mechanics which should be called linear crack mechanics and the latter is the measure of severity in linear notch mechanics. That is, linear notch mechanics is defined as an engineering method which treats the notch problems by elastic stress fields (represented by σ_{max} and ρ) alone similarly as linear crack mechanics is defined as an engineering method which treats the crack problems by elastic stress fields (represented by stress intensity factors) alone.

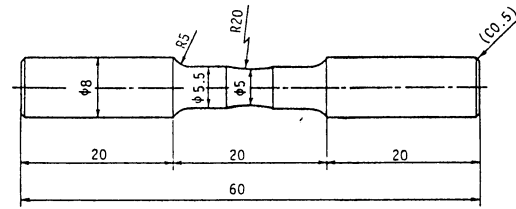
Based on linear crack mechanics and linear notch mechanics, the conditions for causing the same localized damage in two cracked bodies or two notched bodies are shown in Fig. 3. In this figure, only the case of mode I is treated, because the case of the other mode is similar to the case of mode I.

3. Materials and Experimental Procedure

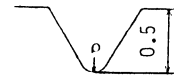
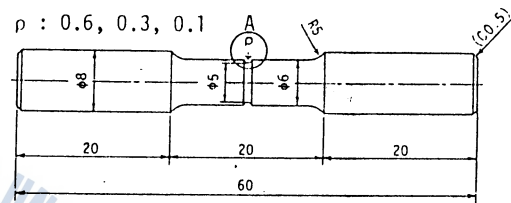
The materials used are aluminum alloy(6061 - T6) and SiC whisker - fiber reinforced aluminum alloy(SiC/6061 - T6) where the whisker - fibers having a diameter of 0.1~1 μ m and the mean length of 5~50 μ m were combined in aluminum alloy with a fiber content of 30% (by weight). Figure 4 shows microstructure of SiC/6061 - T6. As shown in Fig. 4, whisker rich zone and whisker poor zone exist in a layer and whisker - fibers are oriented to the axial direction. Figure 5 shows the shapes and dimensions of plain($\rho=20$ mm) and notched specimens. Rotating - bending fatigue tests of the notched specimens were carried out for three kinds of notch root radii under the conditions of constant notch depth($t=0.5$ mm)



Fig. 4 Microstructure of SiC/6061-T6.



(a) Plain specimen



Detail of A

(b) Notched specimen

Ddimension in mm

Fig. 5 Specimen configurations.

and specimen diameter of the minimum section ($d=5\text{mm}$). Table 2 shows the values of stress concentration factors at a notch root. Plain ($d=5\text{mm}$, $\rho=20\text{mm}$, $K_t=1.04$) and notched specimens were polished with fine emery paper and alumina. Thereafter, aluminum alloy 60691-T6 specimens were electropolished and SiC/6061-T6 specimens were etched to discriminate the whisker existence on the surface easily (etchant : $\text{H}_3\text{PO}_4 : \text{H}_2\text{O} = 1 : 3$).

A rotation-bending fatigue testing machine of uniform bending moment type was used. The stress used in this research is the nominal bending stress at the minimum section. The crack nucleation and propagation process for plain specimen were confirmed from the results of successive observations.

4. Experimental Results and discussion

Figure 6 shows the stress-stain curves in tensile tests of 6061-T6 and SiC/6061-T6. By reinforcing due to the whisker-fibers, the tensile strength and elastic modulus increase, respectively, but the fracture elongation decreases, in contrast. The data obtained from the tensile tests are tabulated in Table 1.

Figure 7 shows S-N curves of plain specimens. As the distinct fatigue limit of these materials did not appear, the fatigue strength at 10^7 cycles for plain specimen (σ_{w0}) was adopted. σ_{w0} for 6061-T6 and SiC/6061-T6 are about 160MPa and 250MPa, respectively. The fatigue crack nucleation and propagation processes for SiC/6061-T6 and 6061-T6 are shown in Figs. 8 and 9. As shown in Fig.8, in the case of the SiC/6061-T6 the fatigue crack is nucleated from the end of the whisker near the boundary between whisker rich zone and whisker poor zone. On the other hand, in the case of the 6061-T6 the fatigue crack is nucleated from the defect and propagates by the shear type.

Fatigue crack growth curves of SiC/6061-T6 and 6061-T6 are shown in Figs.10 and 11.

Figure 12 shows the relation between crack length, l , and relative number of cycles, N/N_f . In the case of the SiC/6061-T6, the fatigue life is determined mainly by the crack propagation of up to about 0.1mm. But in the case of the 6061-T6 the fatigue crack reaches 0.1mm early and the whole fatigue life is controlled mainly by the fatigue crack propagation, as can be seen from Fig.12.

Figure 13 shows S-N curves of the notched specimens for SiC/6061-T6 and 6061-T6. It was confirmed from the observation of the surface state of the notch root after 10^7 cycles that the crack is observed when the notch root radius ρ is 0.1mm for SiC/6061-T6.

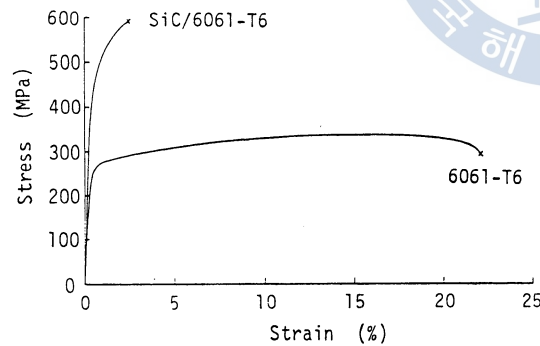


Fig. 6 Stress-strain curves.

Table 1 Mechanical properties of SiC/6061-T6 and 6061-T6.

	E (MPa)	$\sigma_{0.2}$ (MPa)	σ_B (MPa)	σ_{w0} (MPa)
6061-T6	67900	260	335	160
SiC/6061-T6	114800	467	595	250

E : Young's modulus

$\sigma_{0.2}$: 0.2% proof stress

σ_B : Ultimate tensile strength

σ_{w0} : Fatigue strength at 10^7 for plain specimen

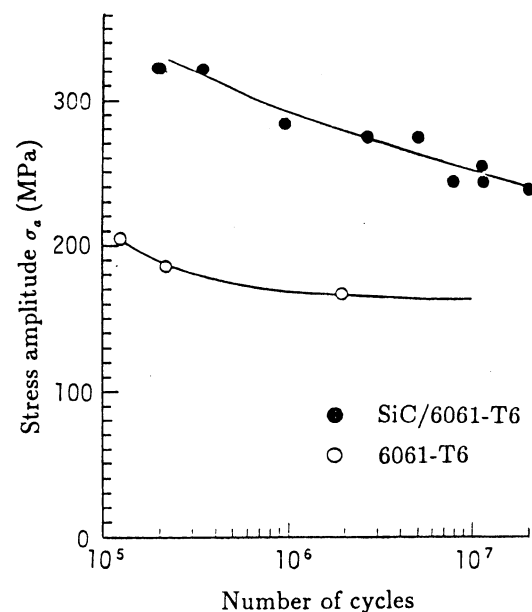


Fig. 7 S-N curves of plain specimens.

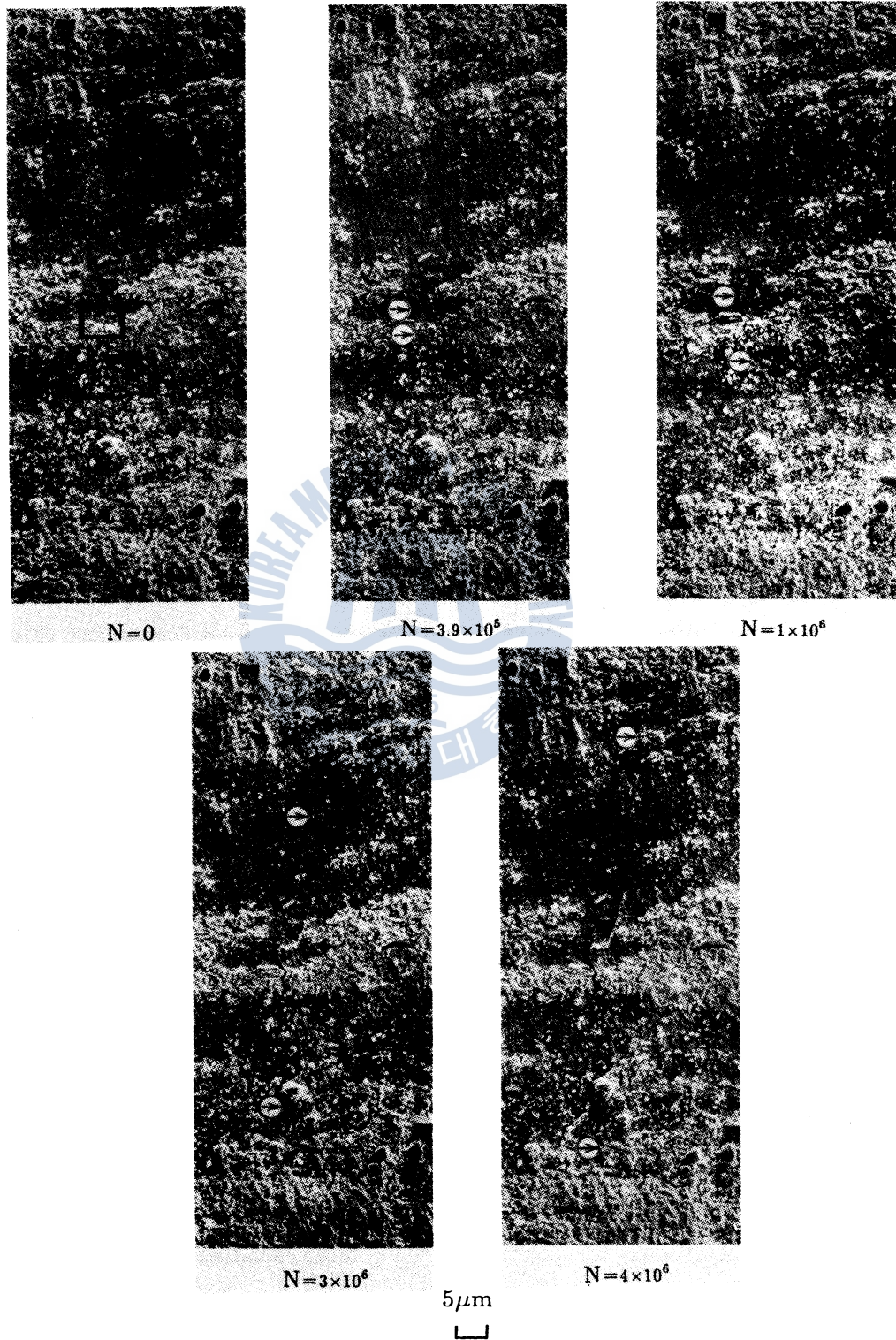
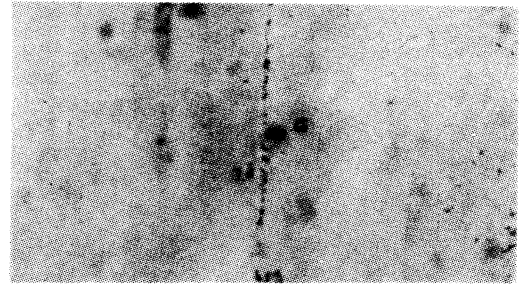


Fig. 8(a) Crack initiation and propagation processes for the SiC/6061-T6.

$N=0$



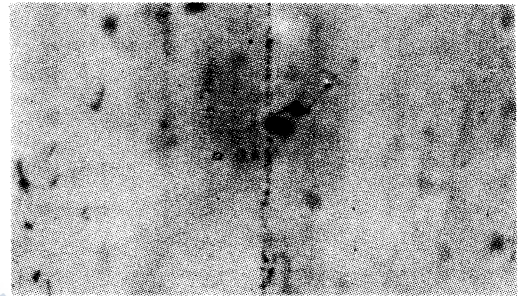
$N=0$



$N=3.9 \times 10^5$



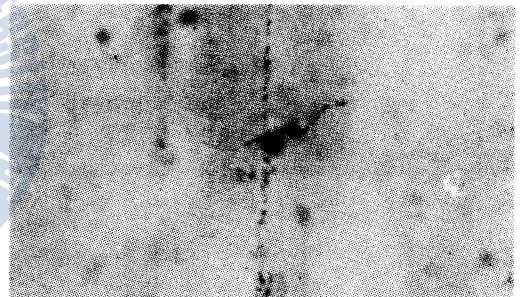
$N=5 \times 10^3$



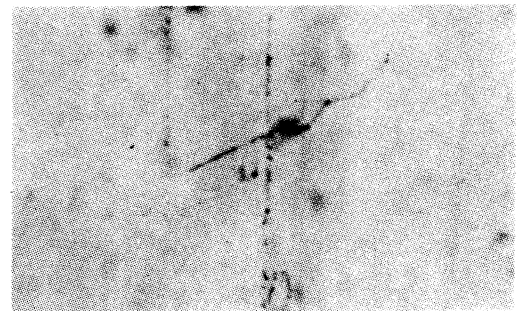
$N=1 \times 10^6$



$N=1 \times 10^4$



$N=2 \times 10^4$



$N=4 \times 10^4$

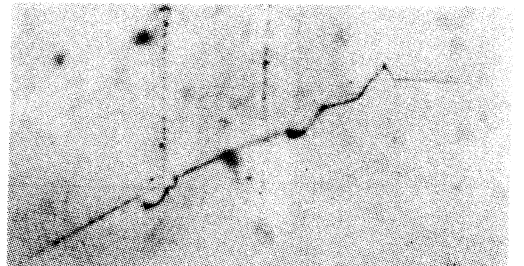


Fig. 8(b) Enlargement of part □ in Fig. 8(a).

Fig. 9 Crack initiation and propagation processes for the 6061-T6.

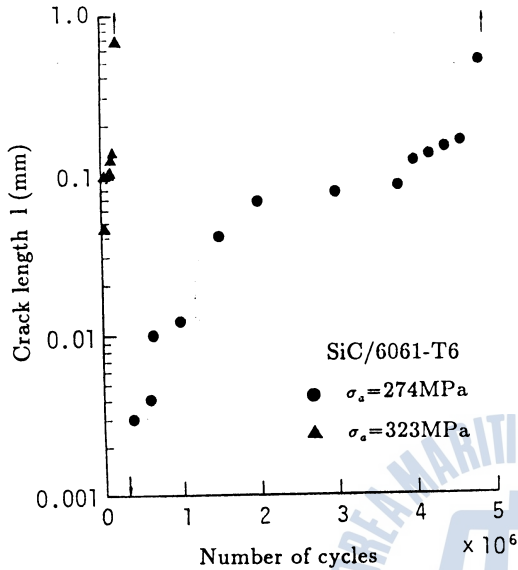


Fig. 10 Fatigue crack growth curves of SiC/6061-T6.

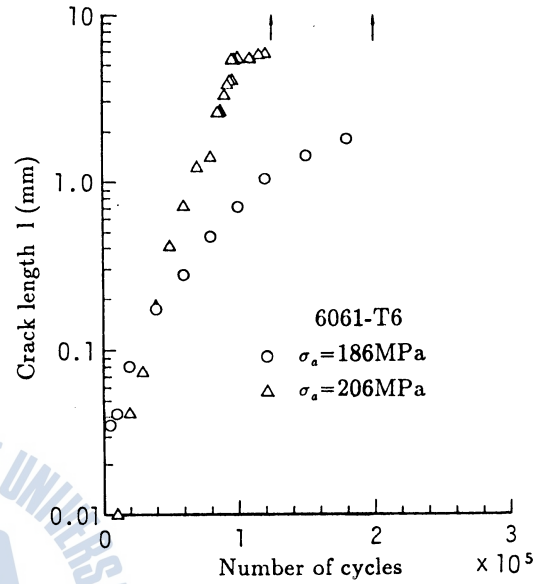


Fig. 11 Fatigue crack growth curves of 6061-T6.

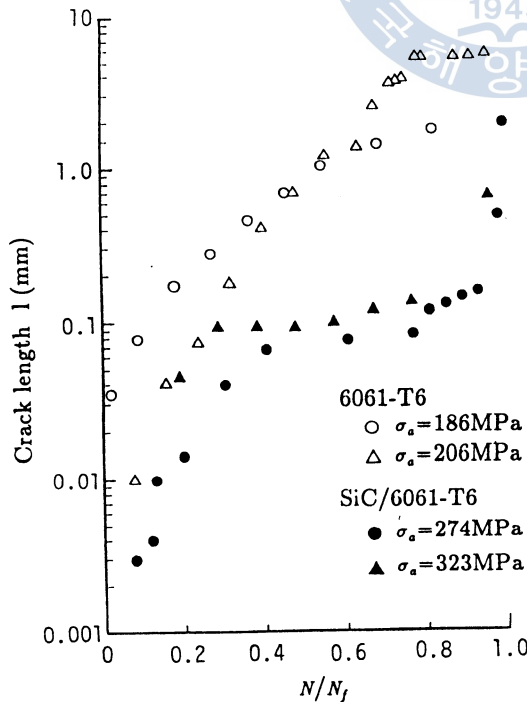


Fig. 12 Relation between crack length l and relative number of cycles N/N_f .

and 0.1mm and 0.3mm for 6061-T6, respectively.

The relation between σ_{w1} or σ_{w2} and K_t is given in Fig.14. The limiting stress for macrocrack initiation, σ_{w1} , is defined originally as the maximum nominal stress(17) under which a macrocrack does not appear along the notch root, but it is very difficult to discriminate the macrocrack initiation in this composite. Thereupon, σ_{w1} is defined in this paper as the limiting stress where the fatigue crack of about 0.1mm observes after 10^7 cycles. And the limiting stress for fracture in the range of macrocrack existing after 10^7 cycles, σ_{w2} , is defined as the threshold nominal stress(19) for crack propagation in the range where a non-propagation crack ex-

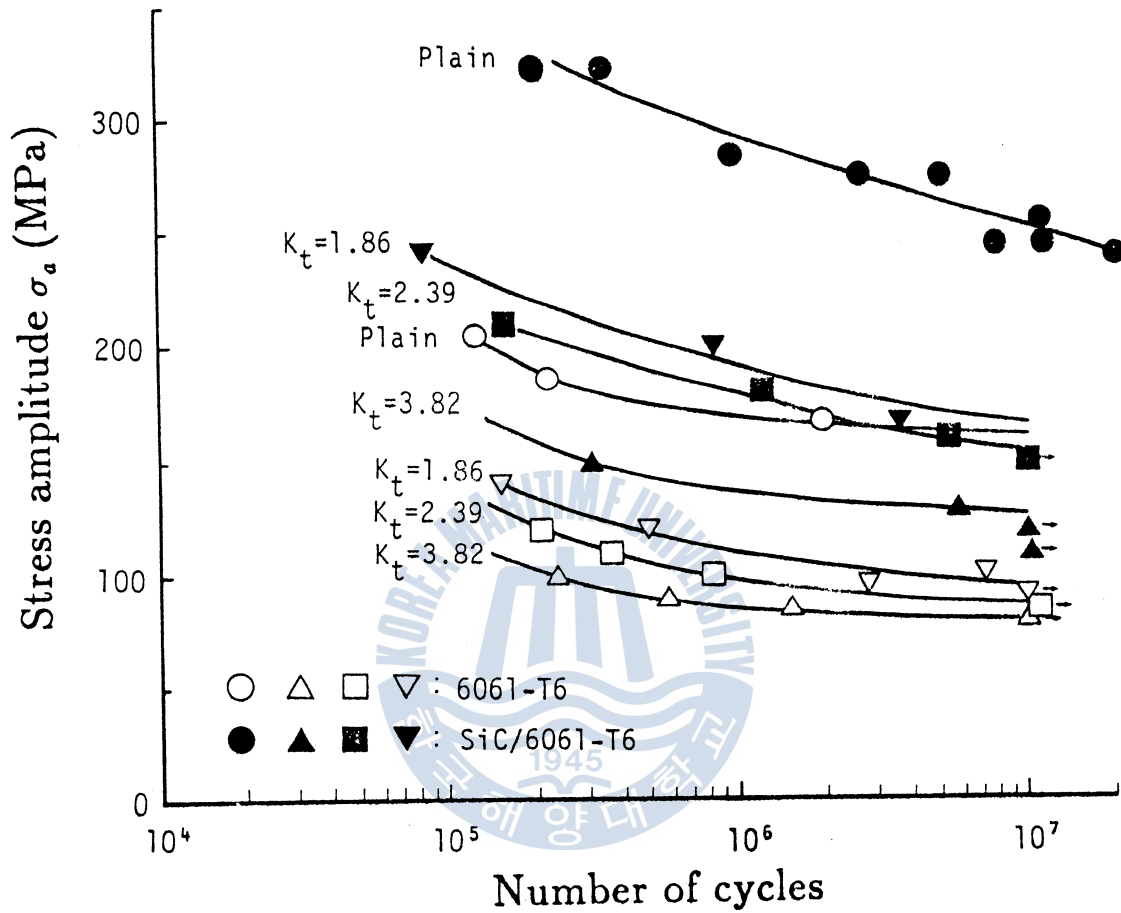


Fig. 13 S-N curves of the notched specimens.

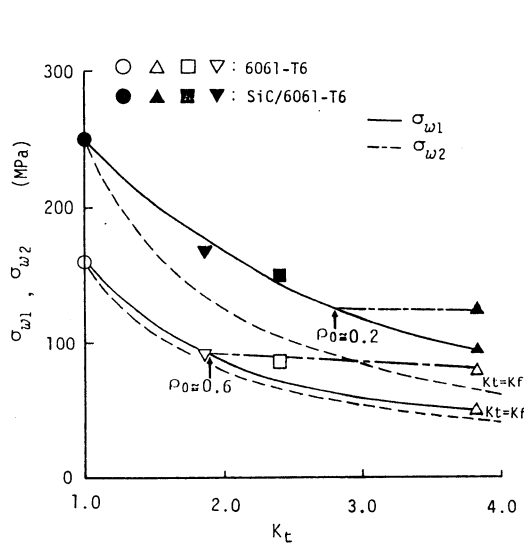


Fig. 14 Relation between σ_{w1} or σ_{w2} and K_t .

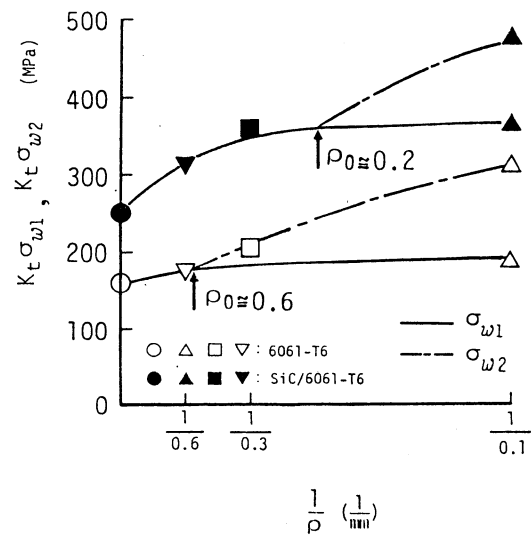


Fig. 15 The plot of $K_t \sigma_{w1}$ or $K_t \sigma_{w2}$ against $1/\rho$.

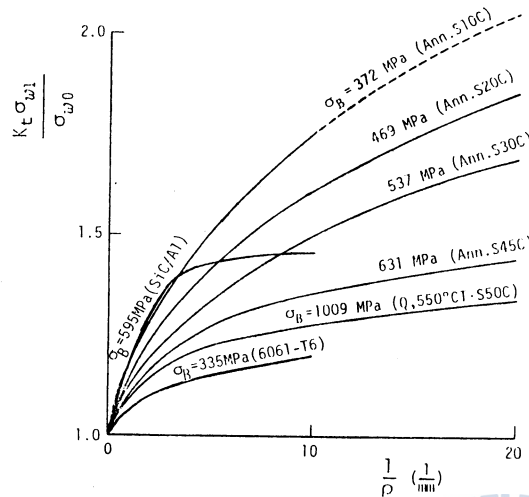


Fig. 16 Relation between $K_t \sigma_{w1}/\sigma_{w0}$ and $1/\rho$.

Table 2 The values of stress concentration factors at a notch root.

Symbols	ρ (mm)	K_t
○ ●	20	1.04
▽ ▼	0.6	1.86
□ ■	0.3	2.36
△ ▲	0.1	3.82

○△□▽ : 6061-T6
 ●▲■▼ : SiC/6061-T6

ists.

The plot of $K_t \sigma_{w1}$ or $K_t \sigma_{w2}$ SiC/6061-T6 and 6061-T6 against $1/\rho$ based on linear notch mechanics is shown in Fig.15. The notch root radius at branch point, ρ_0 , for 6061-T6 is smaller than that of SiC/6061-T6 (SiC/6061-T6 : $\rho_0=0.2\text{mm}$, 6061-T6 : $\rho_0=0.6\text{mm}$).

Figure 16 shows the relation between $K_t \sigma_{w1}/\sigma_{w0}$ and $1/\rho$ for SiC/6061-T6 and 6061-T6. Concerning σ_{w1} , it seems to be insensitive to a notch for SiC/6061-T6, and sensitive to a notch for 6061-T6.

However, $K_t \sigma_{w1}/\sigma_{w0}$ is nearly constant when ρ is smaller than certain value. This situation is shown in Fig.17. It can be considered from the results of Fig.8 that the crack initiation is of the point-initiation type (Fig.8) and the fatigue strength of SiC/6061-T6 is very sensitive to a notch. However, the fatigue strength of SiC/6061-T6 is insensitive to a

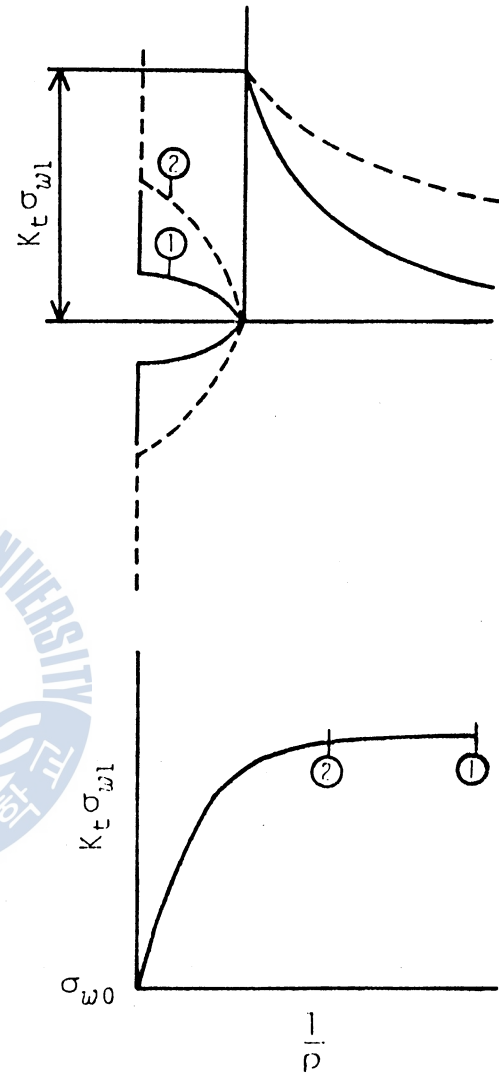


Fig. 17 Explanation diagram.

notch, as shown in Fig.16. This is due to the fact that the fatigue limit of plain specimen was lower than the true fatigue limit because of the statistical factors. Figure 16 is able to be a master curve in the case of steel which does not obtain the influence of the statistical factors, but there is a need to use carefully the master curve in evaluation of the fatigue strengths of the materials which are strongly influenced by the statistical factors.

5. Conclusions

Rotating-bending fatigue tests for aluminum alloy (6061-T6) and whisker-fiber reinforced aluminum alloy (SiC/6061-T6) where the whisker-fibers having a diameter of $0.1 \sim 1 \mu\text{m}$ were combined in aluminum alloy with a fiber content of 30% (by weight) were carried out to investigate the fatigue characteristics of plain and notched specimens at room temperature. The results obtained can be summarized as follows.

(1) In the case of the SiC/6061-T6 the fatigue crack is nucleated from the end of the whisker near the boundary between whisker rich zone and whisker poor zone. On the other hand, in the case of the 6061-T6 the fatigue crack is nucleated from the defect and propagates by the shear type.

(2) It can be considered from the results of Fig.8, that the crack initiation of SiC/6061-T6 is of the point-initiation type (Fig.8) and the fatigue strength is very sensitive to a notch. However, the fatigue strength of SiC/6061-T6 is insensitive to a notch, as shown in Fig.16. This is due to the fact that the fatigue limit of plain specimen was lower than the true fatigue limit because of the statistical factors.

(3) The fatigue strength of an arbitrary notched specimen will be estimated from each master curve rearranged based on linear notch mechanics.

References

- 1) A. P. Divecha et al., J. Metals(1981), 12.
- 2) M. Akiyama, Industrial materials, 31-2(1983), 49.
- 3) S. V. Nair et al., Metals, 30-6(1985), 276.
- 4) H. Fukunaga et al., j. Soc. Mater. sci., 34-376(1985), 64.
- 5) W. A. Logadon and P. K. Liaw, Eng. Fract. Mech., 24-5(1986), 737.
- 6) T. Christman and S. Suresh, Mater. Sci. and Eng., A 102(1988), 211.
- 7) T. Hattori and M. Sakai, Mitsubishi juko Giho, 25-4(1988), 357.
- 8) K. Hirano and H. Takizawa, Trans. Jpn Soc. Mech. Eng., 55-511(1989), 373.

- 9) K. Hirano and D. Nakazawa, Trans. Jpn Soc. Mech. Eng., 55 - 520(1989), 2427.
- 10) C. Masuda and Y. Tanaka, Iron and Steel, 75(1989), 1753.
- 11) K. Hirano, JSME Int. Journal, 34 - 2(1991), 234.
- 12) C. Masuda et al., J. Jpn Soc. Compo. Mater., 17 - 2(1991), 66.
- 13) L. Geng et al., Proc. ICM(Edited by Jono and Inoue, kyoto), (1991), 125.
- 14) G. R. Irwin, fracture I, Encyclopedia of Physics, Edited by S. Flugge, springer Verlag, Berlin (1958), 558.
- 15) H. Nisitani and H. Hyakutake, Eng. Fract. Mech., 22 - 3(1985), 359.
- 16) H. Nisitani, Trans. Jpn Soc. Mech. Eng., 11 - 48(1968), 947.
- 17) H. Nisitani, Trans. Jpn Soc. mech. Eng., 48 - 447(1983), 1353.
- 18) H. Nisitani, Proc. Inter. Conf. on Role of Fract. Mech. in modern Technology, edited by G. C. Sih and H. Nisitani, Elsevier, Amsterdam.(1987), 23.
- 19) H. Nisitani(Edited by), Fatigue strength, (1986), Ohm press.

